Determining the Impact of VAWT Farm Configurations on Power Output

Andrew Barnes*, Ben Hughes

Department of Mechanical Engineering, University of Sheffield, United Kingdom
**Corresponding author: abarnes2@sheffield.ac.uk*

Abstract

The potential for significant increases in VAWT farm performance compared to isolated turbines is well documented and could potentially allow VAWTs to compete in the Wind Energy market. In order to determine the most effective layout based upon both average turbine efficiency and efficient use of area, different configurations which have been shown to offer improved performance such as the 'School of Fish' design alongside new derivative and hybrid designs are compared and optimised using 2D URANS (Unsteady Reynold's Averaged Navier Stokes) CFD simulations. The results show that on a farm scale, the optimised staggered configuration provides the highest array power coefficient for a single wind direction, with a farm design proposed in order to achieve maximum efficiency and results showing increases in array power of up to 80%. Fluid flow mechanisms which cause this improvement are also identified.

Keywords: Vertical Axis Wind Turbine (VAWT), 2D CFD, Wind Farm, Power Coefficient

Highlights

1. Staggered farms offer the highest performance compared to other tested configurations
2. Power increases of ≥80% over isolated turbines can be found in ideal staggered design
3. Mechanism combines Venturi effect, reduction of normal flow, and wake contraction.

Nomenclature

λ	Tip Speed Ratio
ρ	Density (Kg m^{-2})
σ	Solidity
τ	Rotational Speed (Radians/sec)
τ	Torque (Nm)
b	Interference Parameter
C_{PA}	Array Power Coefficient
C_P	Power Coefficient
D	Diameter
P	Power
S	Cross-sectional Area
V	Velocity
V_∞	Freestream Velocity

1. Introduction

With the increasing development of wind energy projects, there has been consequential research into novel solutions and in some cases reviewing older studies and revitalising them using new technology and techniques. VAWTs fall into the latter, with a considerable amount of research conducted in the 1960s and 70s until it was determined that HAWTs (Horizontal Axis Wind Turbines) were the more suitable option with higher efficiencies and lifetimes. During the 21^{st} century however, there has been a renewed interest, particularly spurred by works which have shown significant increases in performance when VAWTs are considered in the farm context [1][2][3]. Given the increasing sizes of farms,

the farm context is becoming a larger influence on wind farm developments. This is enhanced further by the small spacing between HAWTs which is demanded by industry and government subsidies, often as little as 7 diameters between turbines [4] when studies have shown that this can cause severe detriments to farm performance, and even spacings as large as 12D result in a 40% reduction in performance [5]. In contrast, it has been shown that with good farm design, such small and even smaller spacings for VAWTs are not just viable but in fact can be desirable, potentially offering a magnitude increase in power per area compared to an optimised HAWT farm [6]. Though it has also been debated whether this is as valuable as it has been portrayed, given that the space between wind turbines in Onshore wind farms is often used for other purposes such as farming and so is not merely turned into dead space by the farm's existence. For terrain limited farms such as offshore and roof-mounted installations there may still be some merit however.

While much research has been conducted on VAWT farm configurations in the past, each piece has had its limitations. Much of the work relies on simplified point dipole models which cannot fully capture the flow [1][7]. Alternatively an experimental site is used however it could be argued that the value of a single site is limited as results will be dictated by the wind conditions during testing, which may not be representative or apply to other locations. The majority of this research also uses very low wind speeds of 3m/s which would not be applicable to industrial farms where most of the power generated will be from wind speeds in the 10m/s range [8]. Other work using CFD such as Zanforlin and Nishino [3] only considers very small numbers of turbines which prevents the results from being applied to larger farms. There are also very few comparison studies, and where these exist there is a lack of cross-comparability between studies, hence this work compiles these different configurations into one methodology based upon which aspects provide the most accurate results without causing inoperable time requirements[9], and designed to be industrially applicable by using a relevant wind speed.

Several major farm designs exist, with the baseline being the grid formation. Alongside this there are configurations which are reported to improve performance, these include the Staggered, School of Fish, and 2 and 3 turbine Clustered designs as shown in figure 1. While combining the re-

sults of previous literature suggests that a 3 turbine cluster design should be the highest performing, it ignores that the 3 turbine cluster is a special case of the Staggered design with a less efficient use of space due to the larger distance between clusters, and so it is necessary to question whether other special cases exist. Given the mechanisms of fluid flow determined by Zanforlin [3], it is strongly suggested that the high turbine density used by the clustered design can also be applied to the staggered design, creating an even more efficient array. Genetic algorithm led designs are also reported to improve performance in HAWTs [10] and VAWTs [11] however due to the high computational complexity this was not possible to implement when combined with the also computationally complex CFD methodology used.

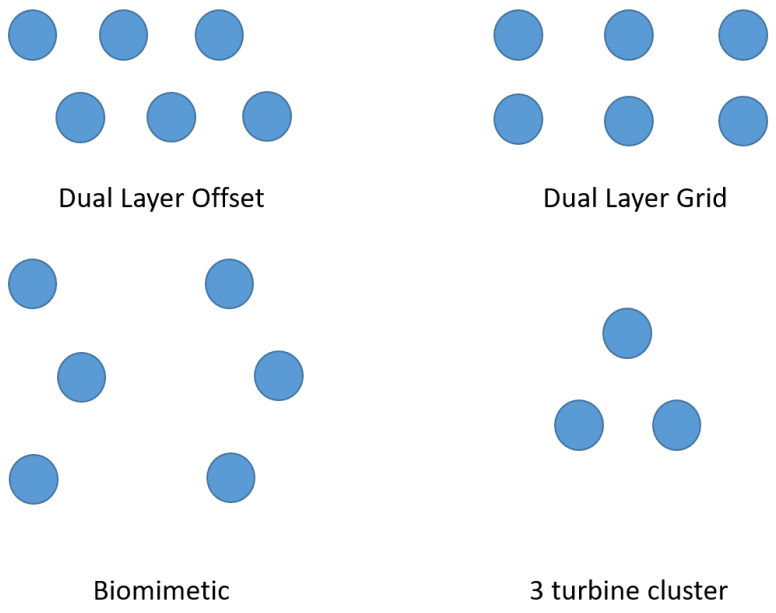

Figure 1: Examples of Configurations for a 6 Turbine Farm

The turbine design considered was a genetic algorithm optimised design by Carrigan using a NACA0023.7 aerofoil with 3 blades and a very high solidity of 0.883 [12]. As a fully dynamic system was used rather than a fixed tip-speed ratio as in most other studies, the high solidity allowed for a self-starting turbine [13]. While the high solidity decreases

off-design performance in exchange for higher efficiency [14], this is offset by the higher thickness of the aerofoil which increases performance in this area [13]. While such a high solidity is often considered as inapplicable to the real world, there are examples of commercially available turbines with even higher solidity values [15]. For sake of comparison, a more typical solidity turbine with σ=0.120 was also produced in order to consider any possible effects on the results. The system was chosen to use a chord length of 1m and diameter of 3.4m, which corresponded to a 10m blade length and VAWT height in the 2D CFD, as this provided a good intermediary between smaller scale VAWTs, such as the Windspire, and industrial scale turbines. For the low solidity turbine, the same aerofoil and measurements were used with the exception of a chord length of 0.136m. Using this turbine geometry, a set of farm geometries were produced so that their performances could be analysed using CFD.

2. Methodology and Validation

2.1. Model Set-up

Table 1: CFD Solver Settings

Time	Transient
2D Space	Planar
Pressure-Velocity Coupling	PISO
Gradient	Least Squares Cell Based
Pressure	Second Order
Momentum	Second Order Upwind
Turbulent Kinetic Energy	QUICK
Specific Dissipation Rate	Second Order Upwind
Intermittency	Second Order Upwind
Momentum Thickness Re	Second Order Upwind
Transient Formulation	Second Order Implicit

All simulations completed for this study were performed in ANSYS Fluent 18.2. Previous literature by Lanzafame and Danao has shown that the Transition SST turbulence model is a core requirement for achieving the most accurate results for VAWT performance when using URANS for 2D CFD [9][16], outperforming SST k- ω as used in many other studies

[27][17][18]. A Pressure based solver was used and all other settings are described as in table 1.

2.2. Boundary Conditions

Table 2: Boundary Condition Settings

Condition	Settings
Inlet	Velocity inlet with a velocity of 10 m/s. Turbulent Intensity and Turbulent Viscosity Ratio remained at their defaults of 5% and 10 respectively.
Outlet	Pressure outlet with a gauge pressure of 0 Pa as there is no forced pressure differential across the system.
Symmetry	Applied to side walls
Domain	Air at default settings (Sea Level).
Walls	The blades were modelled as rigid bodies as the Fluid-Structural interactions would be insignificant.

2.3. Meshing

Production of a good mesh is essential for an accurate and functional simulation as a coarse mesh can provide inaccurate results and a mesh with highly skewed cells can cause the results to become divergent.

The 'Proximity and Curvature' size function was chosen in order to ensure a high mesh density around the blades of the turbine. Relevance centre was set to medium, and 'Faces and Edges' was chosen as the Proximity Size Function Sources.

Global maximum face size was chosen to be 0.10m and an additional maximum face sizing of 0.04m was applied to the rotating core regions. An element size of 0.01m was also applied to the blade surfaces, with this set to 0.001m instead for the low solidity turbine to approximately match the same number of surface elements.

Inflation was applied to the turbine blades with a maximum of 16 layers allowed. This provides a finer, more structured mesh around the

blades, which is necessary as flow in these regions will have the greatest effect on the system.The inflation layers can be seen in figure 3.

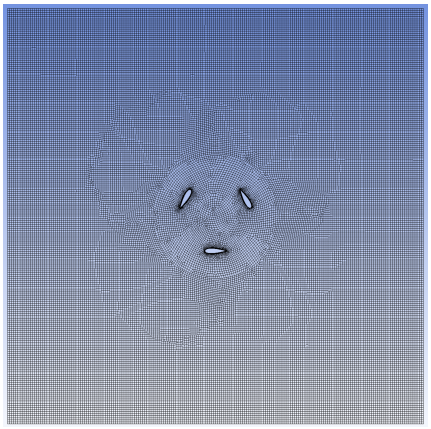

Figure 2: Mesh and Domain Geometry

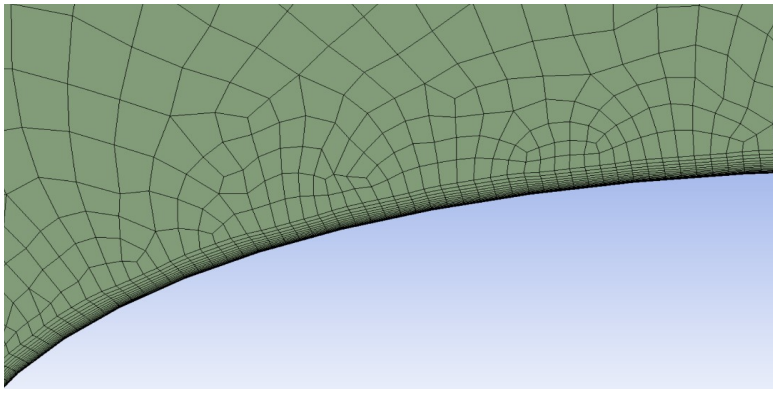

Figure 3: Inflation layers along the VAWT blade surface

This method resulted in some poor characteristics in the mesh with a max Aspect Ratio (AR) of 55.2, however these cells occurred in the boundary layer so the high AR is expected and adequate for good overall performance. Outside of the boundary layer the maximum AR was less than 6.53 as shown by the mesh metrics available in ANSYS Meshing.

The maximum skewness produced was 0.77824 however when the mesh was imported to fluent and the "Improve quality" function was run it en-

abled a reduction to 0.248 which is excellent. The average Skewness was 0.06 which is excellent and Y+ values were less than 1 which is necessary for good performance with SST models. Orthogonal quality was a minimum of 0.27 which is acceptable and an average of 0.988.

2.3.1. Dynamic Mesh

The walls between the rotating cores and the rest of the control domain were set as interfaces to allow the fluid to flow through them and thus rotate the turbine and produce a wake downstream.

The Dynamic Mesh methods of Smoothing, Layering, and Remeshing were enabled, where the Smoothing method was set to Diffusion, Layering was left at default, and for Remeshing the minimum and maximum length scales were set to the original value and maximum skewness was set to 0.7.

The rotating cores were then setup using the 6DOF (6 Degrees of Freedom) solver in Fluent where only one degree of freedom was allowed: rotation around the Z axis.

2.4. Power Calculations

Carrigan [12] established a method for calculating average torque from the data collected in FLUENT, where t_0 is the beginning of the rotation with minimum torque, and t_n is the data point before the next point of minimum torque, the end of the revolution [12]:

$$\tau_{avg} = \frac{\Delta t}{2(t_n - t_0)} \left[\tau(t_0) + 2 \sum_{i=1}^{n-1} \tau(t_i) + \tau(t_n) \right] \tag{1}$$

However during testing this tended towards zero as in steady state the oscillation of torque will tend around zero as the average rotational speed is no longer increasing, and a more suitable equation was devised:

$$\tau_{avg} = \frac{\Delta t}{2(t_n - t_0)} \left[2 \sum_{i=1}^{n} (\tau(t_i) - \tau(t_0)) \right] \tag{2}$$

The individual torque values τ_i were recorded using the moment report function in FLUENT, this produced a list of the torque values at

each interval which was then input into MATLAB to calculate the average power. A time step of 0.005 seconds was set during this data collection stage and this was run for at least 120 steps until 3 peaks of equal magnitude were seen, which enabled the capture of a full revolution of the slowest rotating turbines. The ω values were output by FLUENT's dynamic mesh utility.

Mechanical power only on the turbine was used and losses due to friction and windup were not considered.

The power values for all turbines in the farm were then averaged to produce P_{avg}. This was then divided by the power of the airflow available to an isolated turbine as calculated using equation 3.2 to produce the Array Power Coefficient:

$$P_{avg} = \frac{1}{n}\sum_{i=1}^{n} \tau\omega \tag{3}$$

$$P_{wind} = \frac{1}{2}\rho V_{\infty}^{3} S \tag{4}$$

$$C_{AP} = \frac{P_{avg}}{P_{wind}} \tag{5}$$

It is important to use the array power coefficient with P_{wind} rather than localising to each turbine in order to ensure comparability, as the local velocity will vary for following turbines due to wake effects of leading turbines, and so averaging the local C_p would provide incomparable results.

2.5. Verification

2.5.1. Residuals and Convergence Criteria

Residuals are measures of the difference between one iteration and the previous iteration and act as a measure of convergence. For the first 40 seconds of simulation time, the amount of time required to ensure the turbines had reached steady state, the convergence criteria required residuals to be set to 10^{-3} for 6+ turbine simulations and 10^{-4} for smaller farms to ensure good accuracy while allowing for reasonable compute times. After this the size of the time steps were reduced in order to ensure greater accuracy and the residual requirement for convergence was reduced to 10^{-4} for simulations of 6 turbines and above, and 10^{-5} for any simulations with fewer than 6 turbines.

2.5.2. *Mesh Analysis*

An appropriate Mesh Density, measured by cell count must be found in order to ensure a good balance between computational time and error from the converged value. For a single turbine it was found that 45,000 cells were sufficient to minimise error and for a 4 turbine simulation 160,000 cells was enough to reach the converged values. Hence it can be concluded that the meshes used should require at least 40,000 cells per turbine.

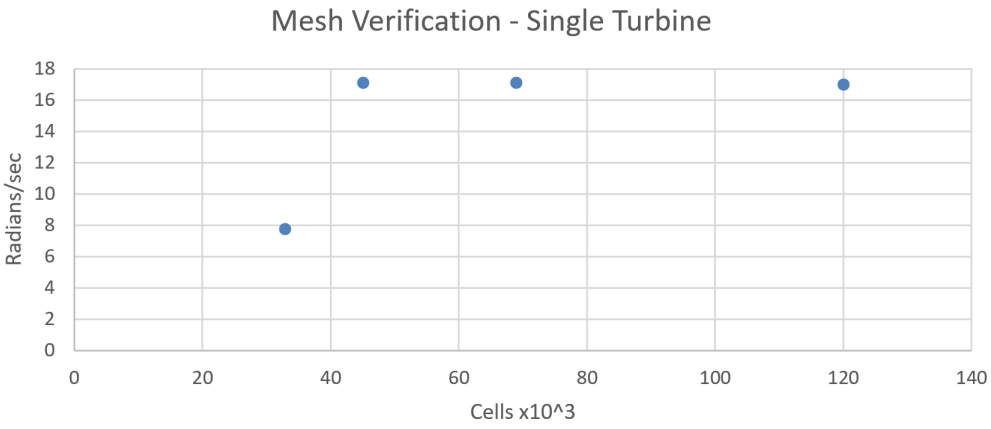

Figure 4: Single Turbine Mesh Verification - Cells Against Rotation Speed

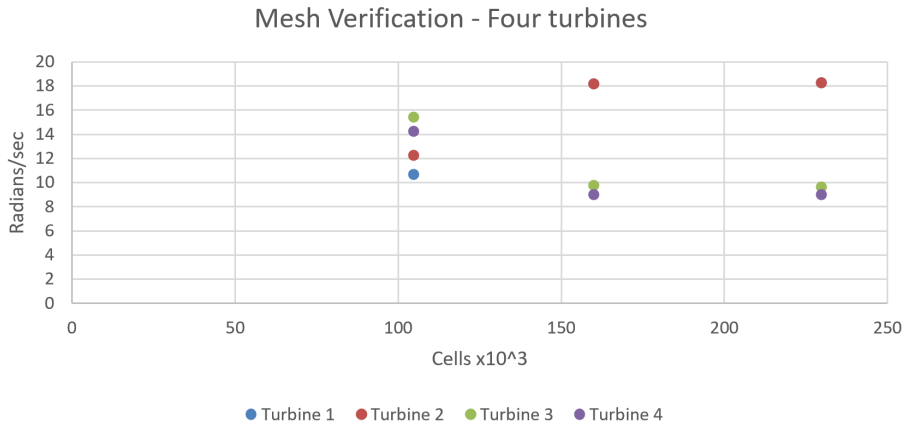

Figure 5: Four Turbines Mesh Verification - Cells Against Rotation Speed

The y+ values were also set to be less than 1, a requirement for good performance of the Transition SST model.

2.6. Domain Dimensions

2.6.1. Rotating Core

A rotating core was placed around the turbine to allow for rotation in the dynamic mesh, and so the VAWT will spin as a result of the airflow. The rotating core was chosen to have a 5m diameter, or 1.5D, as suggested by Rezaeiha [19].

2.6.2. Inlet Distance

An inlet distance of 3D giving a power coefficient of 0.252, an overestimate of 2.5% over the converged condition, was considered sufficient.

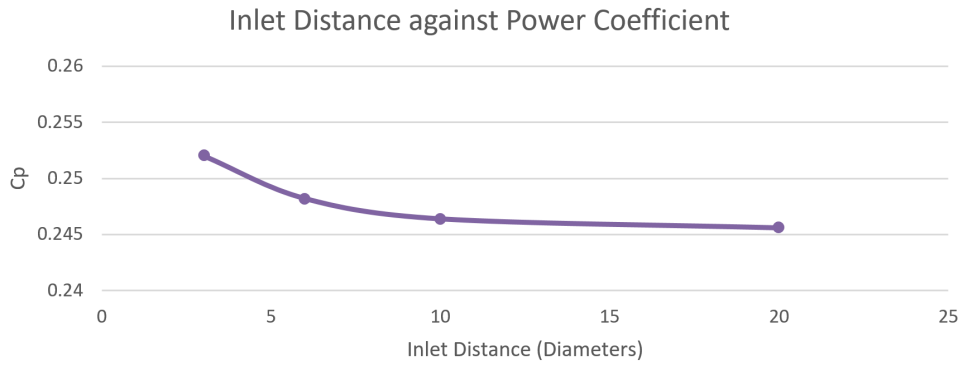

Figure 6: Effect of Inlet Distance from centre of turbine on Power Coefficient

2.6.3. Outlet Distance

It was found that an outlet distance of 6D was sufficient, giving a power coefficient of 0.254, an overestimate of 1.6% compared to the converged value.

2.6.4. Domain Width

Lanzafame used a width of 4D for a single turbine by using symmetry, or 2D on either side from the centre of the turbine [9]. Due to the interference caused by additional turbines a width of 6D, or 3D from the centre

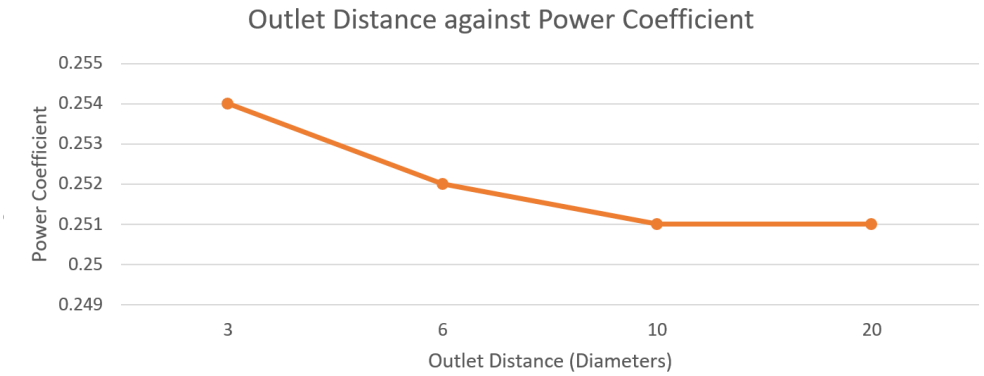

Figure 7: Effect of Outlet Distance from centre of turbine on Power Coefficient

of the turbine when farms were analysed, was chosen with symmetry implemented.

2.7. Compliance with Betz's Law

Due to the nature of the work in trying to increase the farm power coefficients to very high levels it is necessary to ensure that all turbines comply with Betz's limit which states that a Wind Turbine cannot remove more than 59.26% of the power from an airflow. [20]

This was measured by placing a horizontal line, of equal length to the diameter of the turbine, 5m ahead of the centre of each wind turbine to measure V1, and another line 5m behind for V2, then measuring the velocities along these lines. The velocity was then used to calculate the power input and output from the turbine and it was found that all cases were compliant with Betz's limit with a max value of 0.5923. Note that this does not describe the efficiency of the turbine itself, only the power lost from the airflow as a result of the turbine's interference.

2.8. Validation

2.8.1. Validation of 2D model

The simplicity of the H-Bladed Darrieus VAWT design allows for a 2D model to be produced without compromising the model, for example blade rotation is retained alongside the consequent wake effects. Lanzafame compared CFD model procedures to determine which would produce the most valid results and found that the Transition SST model provided good agreement with experimental data for a NACA 0015 based

H-Darrieus Turbine [9]. Other studies have also shown good agreement which suggests the 2D model is valid across different turbine designs and so experimental validation for the exact turbine design used is unnecessary [17][21][22].

2.8.2. *Validation of Proposed Methodology*

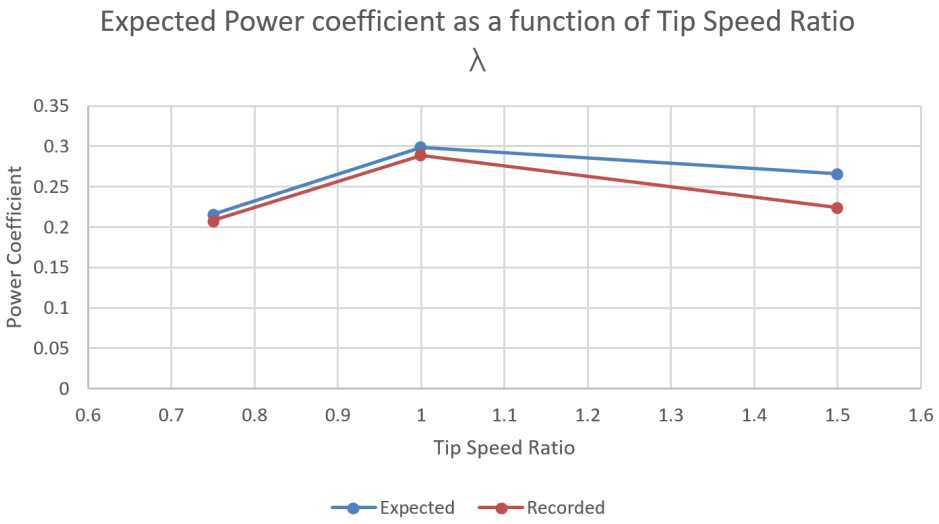

Figure 8: Comparison of tip speed ratios for the expected and recorded power coefficients

It is also necessary to compare the results to those found by Carrigan [12] to ensure that they have agreement. Some difference is expected as shown by Chowdhury [23] due to Carrigan's use of the Spalart-Allmaras model in contrast to the use of Transition SST for this study. Under Carrigan's study, at λ=1 it is expected that C_p=0.4, and when adjusting for this, using the results from Chowdhury [23] and Lanzafame [9], it is found that the Spalart-Allmaras model produces approximately a 34% overestimate in C_p compared to Transition SST, and so C_p=0.299 is expected. During testing a value of 0.289 was found showing good agreement.

The setups for both studies vary in ways other than just the turbulence model, for example Chowdhury assesses λ=3.2 [23] while Lanzafame considers from 0.5 to 1.5 [9], so this explains the difference between the tested value and the experimental result. A comparison between the expected and recorded results is shown in figure 8. It can be seen that there is good

agreement at lower tip speed ratios however at higher tip speed ratios they begin to diverge. As Lanzafame's study showed a greater overestimate between the Transition SST model and the experimental results at higher tip ratios, this is a good result as this showing demonstrates that the expected overestimate will be reduced compared to expectations.

3. Results

3.1. Flow Visualisation

By inspecting the dynamic pressure and velocity contour maps of the farm it is possible to visualise how these results have come to occur. As shown in figure 9, to the sides of the turbine wakes are regions of increased wind speed. This allows for the following turbines which are placed inside these regions of high dynamic pressure to have a much greater power output while not breaking Betz's limit.

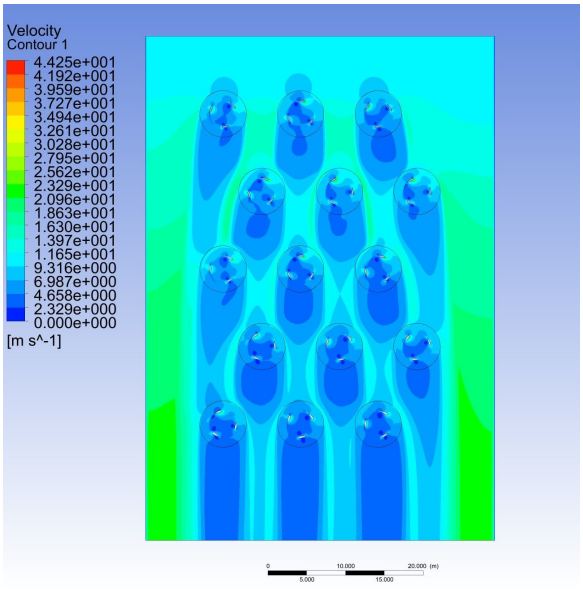

Figure 9: Velocity contour map for a 3x5 farm with spacing x=5, y=10

In the simulation run to produce figure 9 it was found that the absolute wind speed in these regions was 14.5m/s on average across a 1D long line compared to the 10m/s inlet condition. Due to the cubic relationship

between velocity and power this results in a 205% increase in power in the airflow in the path of the turbine, hence why for the optimised farm design it was possible to find turbines in the second row with as much as a 181% increase in power output over the baseline isolated turbine. It can also be seen in figure 9 that these high velocity regions exist in following rows, allowing for further following turbines to receive a power boost also.

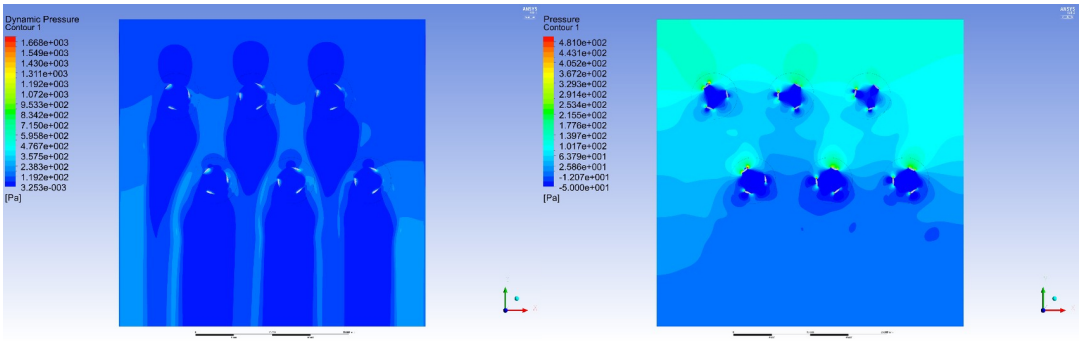

Figure 10: Dynamic and Static Pressure Contour maps for the Optimised Farm

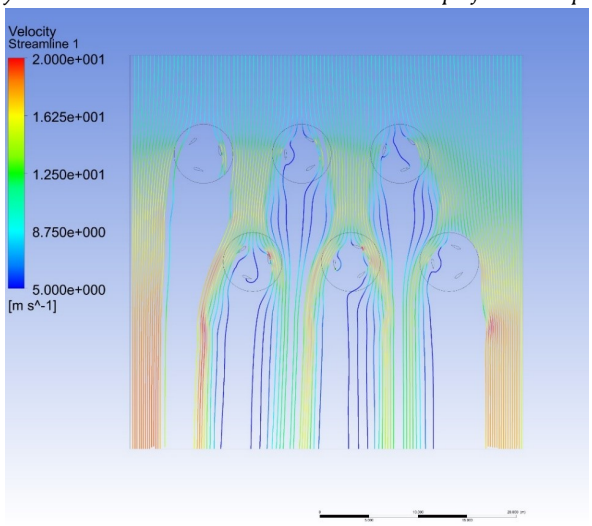

Figure 11: Velocity Streamline map for the Optimised Farm

This occurs due to the Venturi effect which results from the conversion of static pressure into dynamic pressure when flow is constricted, in this case between the turbines. Figure 10 shows the increase in dynamic pressure between the wakes of each turbine, and the corresponding decrease

in static pressure occur in the same regions as expected with the Venturi effect.

The mechanisms discovered by Zanforlin [3] were also confirmed as seen in figure 11 which demonstrates the velocity streamlines, with clear wake contraction and y velocity suppression relative to the blade. The wake contraction can also be seen in figure 9.

To test this a V shaped farm comprised of 5 turbines was created and simulated as shown in figure 12. From the results it was found that the middle layer of turbines, which were only subject to this action from a leading turbine on one side, produced significantly less power than the final turbine and hence two leading turbines are required, one on either side of the turbine of interest, in order to get the greatest performance increase from the effect.

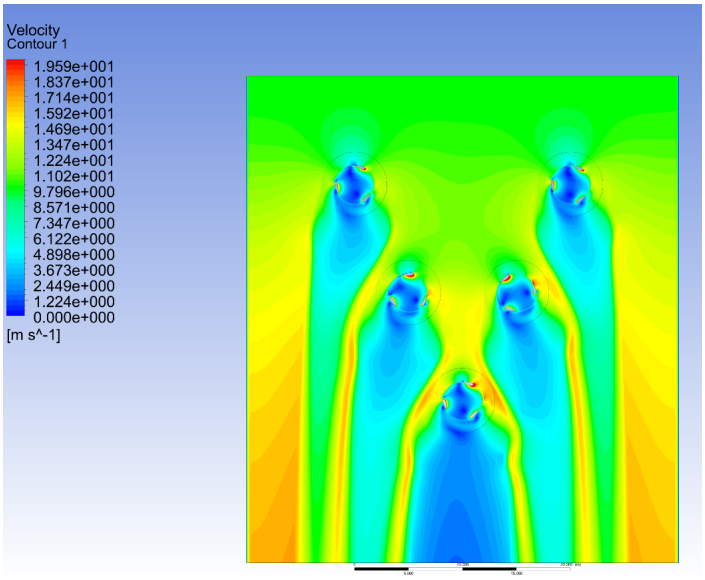

Figure 12: Velocity contour map for a V-shaped farm of 5 turbines

3.2. Isolated Turbine

A single turbine scenario was run and found a power output of 5247.9W, corresponding to a power coefficient of 0.252. This will act as one of two baseline values to compare other results to, where the other will be performance in the grid condition.

3.3. Large Farms

An initial grid of 16 turbines in a 4x4 configuration was run for the grid condition and found that the first row of turbines performed on par with the isolated turbine but severe performance reductions were seen in each following layer of turbines. While it's clear that the performance losses become less severe with each following layer, it can also be seen that there is a severe detriment to performance after the first layer. Interactions between columns were negligible with similar performance in each turbine within a row.

This was repeated for the offset grid/hexagonal with the same number of turbines in a 4x4 configuration, and 'School of Fish' configurations albeit using a 9 turbine farm in a 3x3 configuration. The first layer in both configurations again showed performance on par with the isolated turbines, however it was found that the second layer had a substantial increase in power compared to the first layer. This effect was more prominent in the offset grid design with turbines producing an average of 12.5kW compared to 10kW in the 'School of Fish' configuration. In the third layer it was found that turbines which were exposed to a more open flow of air, e.g. the leftmost turbine in the offset grid configuration produced up to 49.7% more power than those which were more closed off. These results were replicated in the 'School of Fish' design with similar performance across the layer albeit a smaller 18.8% power production advantage for the leftmost turbine, suggesting the spacing between each column pair should be larger than the guidelines provided by Whittlesey [7]. It should be noted that the third layer in the offset grid design still retained a 16.9% performance advantage over the equivalent Biomimetic row, and the lowest power turbines in the offset grid third row produced 8% more power than the equivalent in the Biomimetic design.

This performance difference is equivalent to 3.3% of the baseline isolated turbine performance for a 3x3 farm which can be considered negligi-

ble compared to the 21-30% seen in the second row. It can be extrapolated that this would be even lower for any further following rows, and so it can be concluded that a double row farm is sufficient in order to compare performance of the configurations.

From inspection of the offset grid and Biomimetic designs, it was decided that a width of 3 turbine columns or column pairs would provide a good representation of the performance of larger farms by providing a higher weighting to second row turbines which were preceded by leading turbines on both sides, these can be considered to be inner turbines as they are situated towards the inside of the farm. A width of 2 would provide equal weighting to inner and outer turbines so would provide a poor representation of a larger farm, whereas a width of 4 would result in a large increase in computational cost. As a result it was decided that farms with a 3x2 configuration, for 6 turbines in total, would be used.

3.4. Six Turbine Farms

An initial 3x2 grid configuration with 10m spacing was run in order to provide a second directly comparable baseline in addition to the isolated turbine. An array power coefficient C_{AP} of 0.131 was found, or a 48% reduction compared to the isolated baseline. The grid was also simulated using alternating turbine directions and no significant difference was found in the power coefficient with C_{AP}=0.133

A simulation was then run for the 'School of Fish' condition with c=4D=13.6m, b=c/4=2D=3.4m, a=b/0.3=11.33m, or a spacing of x=3.4m, y=11.33m for each line of turbines giving a result of C_{AP}=0.356 for an improvement of 41.2% over the isolated turbine condition and 271.8% over the grid condition.

For the Staggered condition with a spacing of x=5m, y=10m it was found that C_{AP}=0.425, a 68.8% improvement over the isolated turbine baseline and 324.4% over the grid baseline. This represents a significant improvement over the Biomimetic design. The Staggered farm was simulated again using alternating turbine directions and as with the original grid design no significant difference in power production was found.

A 2 Turbine Cluster based farm was run using the guideline inter-turbine spacing of 1.5D=5.1m, with a horizontal inter-cluster spacing of

4.5D and vertical spacing of 2.65D to match the density of the Staggered and Grid conditions. Due to the discrete nature of the Clusters this was considered in both 4 turbine/2 layer, and 6 turbine/3 layer forms. The 2 layer form had Cp=0.383 while the 3 layer configuration had Cp=0.323.

Two additional farms which used hybrid designs were implemented. The first was based upon the offset grid design albeit with the horizontal distance x=6.8m as used in the Biomimetic design. This produced a reduced C_{AP} of 0.314. The second hybrid design used the Biomimetic design as the foundation, but used the distance between rows that had been used for the grid and offset grid, 10m. This resulted in C_{AP}=0.380 which is significantly higher than the original fish school design as recommended by Whittlesey [7], however still considerably lower than the Staggered design.

From these results it is clear that the Staggered design would become the dominant basis of any design produced by a guided optimisation procedure as it offers a considerable advantage over the guidelines for other established designs.

3.5. Gradient Based Optimisation

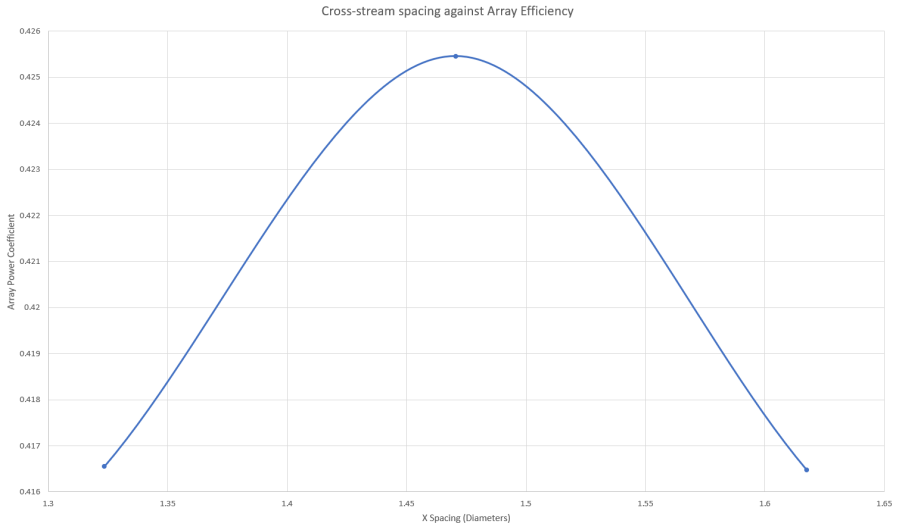

Figure 13: Optimisation of cross-stream spacing on total farm power output

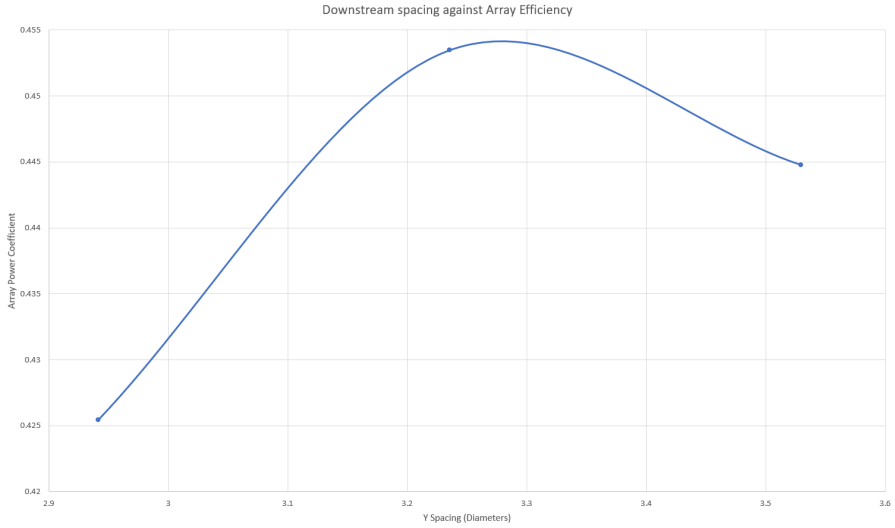

Figure 14: Optimisation of Downstream spacing on total farm power output

The Staggered design was chosen as a basis to run a Gradient-based optimisation due to its high performance. There are two variables which were optimised by iterating simulations using different distances to find the peak value, Cross-stream spacing in the x direction and Downstream spacing in the y direction. The results of this are shown in figures 13 and 14, where the optimum Y spacing occurs at 3.2D (11m) and the optimum X spacing occurs at 1.47D (5m) with an array power coefficient C_{AP}=0.453.

3.6. Low Solidity Turbine Farms

A simulation was run where the turbines in the optimised condition were replaced with the σ=0.12 turbine. From the results, an array power coefficient of 0.355 was found for a 17.2% increase over the isolated Low Solidity Turbine. However this is also a 21.6% reduction compared to the High Solidity case.

3.7. Discussion

3.7.1. Performance Comparison with other VAWT Farms

From the results it is clear to see that special cases of the staggered formation offer the best performance under industrially applicable conditions. The optimised design resulted in an 80% increase in performance

over the isolated turbine condition and 346% over a high density grid condition. While the guideline 'School of Fish' and Clustered designs, alongside Hybrid designs also show significant improvements over the isolated and grid conditions, they still underperform compared to the optimised staggered design.

By comparing to the GA optimised configurations by Bons [11] we can see that there are some similarities in that they also take advantage of staggering, albeit in a less organised way. As stated earlier, the 3 Turbine clusters of Hezaveh [2] are also a special case of staggering.

3.7.2. Performance Comparison with HAWT Farms

In [24] it was found that for a set of three identical in-line HAWTs using a spacing of 3D which is equivalent to that used in this study, with $C_{p,max}$=0.462, the leading turbine had a $C_p/C_{p,max}$ of 1 while the second and third turbines had values of 0.262 and 0.190, providing C_p values of 0.121 and 0.088 respectively. This clearly shows a large performance drop-off when using such small spacing between HAWTs, however this is a worst case scenario and in practice farms will be designed to minimise the time spent in this situation.

For this situation it is necessary to consider [5] which investigates larger spacings between turbines, finding spacings of 12D still carry a highly reduced $C_P/C_{p,max}$=0.6. For a spacing of 3D it is highly likely that there will be a turbine directly downwind within 12D, meaning that even in a best case scenario there are likely to be considerable performance losses in following turbines. As a result of this it is highly recommended against HAWT farms having such small spacing when in a grid configuration.

[10] has shown that for a single wind direction it was possible to achieve an overall farm efficiency of 95% of $C_{p,max}$, corresponding to an array coefficient of 0.418 assuming $C_{p,max}$=0.44 as per the LW 8MW reference turbine based upon the Vestas V164-8MW is normal for HAWTs [25]. For comparison, adjusted for mechanical and generator losses as determined by [20], the optimised VAWT farm would have an array coefficient of 0.417. However Mosetti's configuration required a density of 1 turbine per $104D^2$. In comparison the optimised VAWT solution had a density of 1 turbine per $18.1D^2$. These can then be converted into power coeffi-

cient density =Cp*Turbine density, resulting in $0.00402/D^2$ for Mosetti's HAWT farm and $0.0230/D^2$ for the VAWT farm. While this doesn't meet the magnitude increase in power density suggested by Dabiri [6], it has implications for development of wind farms on space limited sites.

3.7.3. Limitations

Limitations arose from the use of 2D CFD to complete the study which can result in overestimates of power production in comparison to the experimental results. This inaccuracy is difficult to avoid when using CFD however as 3D CFD has been shown to produce underestimates [27]. It is also found that both perform worse in the high tip speed ratio conditions used here with λ=3.6 as the highest result. The lack of 3D simulations also prevents accurate prediction of the wake as flow mixing from the vertical axis is not accounted for. It should be noted that the rate of the wake contraction caused by the Staggered configuration in comparison to an open wake suggests that the flow mixing effects will be negligible for such high density farms, as can be visualised in figure 9. Rezaeiha [15] showed that recovery of streamwise velocity on the VAWT's upwind side of the wake is significantly overpredicted by the Transition SST turbulence model used in this study, which will have an impact on the performance of the local flow mechanism.

The high computational cost of the methods used make it difficult to optimise these configurations on a consumer or even workstation level computer when large farms are considered. For very large arrays of 100+ turbines such as the London array it would be necessary to have a considerable amount of computational power and time available, particularly if the optimisation method was changed. Within this study it prevented the analysis of varying wind speed and direction scenarios.

The use of a single turbine design means the results of this study may not be applicable to other designs. Using the Straight H-Bladed Darrieus design will produce different wakes to the Helical bladed and Standard Darrieus designs. The study also doesn't account for scale, where the results found may change for larger industrial sized turbines.

The high solidity value of the turbine also had an effect, with simulations on a farm using the low solidity turbine showing little interfer-

ence between turbines, but also much lower benefit from the mechanisms. While there was a considerably lower increase in power coefficient, this may be partly due to the configuration not being re-optimised, and further testing is needed, however given that indicators of the Venturi effect are not visible, it is clear that this mechanism is still responsible for the high performance improve present in the Staggered design. In addition, this test used a turbine which was high solidity by high chord length rather than high number of blades, and so it would need to be considered which one of these results in greater farm performance as it could have a considerable impact on the turbine cost.

By only testing a single wind direction, this prevents the results from being fully applicable to a real world situation. However the suppression of the horizontal velocity component alongside the wake contraction suggests that there will be flow redirection between the first and second layer of turbines, providing a more favourable condition for the second layer of VAWTs rather than would be expected in a single column model. While this will not provide the same high efficiency as the single direction design, it will be advantageous compared to following turbines laying in more of the wake as would otherwise be expected. The simple and uniform nature of the design also allows for an easy modification in order to achieve higher off-design performance. By curving the layers it is possible to provide near optimal performance for a small range of wind directions. This could be highly effective as in nature, wind direction tends to be concentrated towards a certain direction or its anti-direction, particularly at sites with the high wind speeds which are more suitable for wind energy solutions.

4. Conclusion

For this study, a series of 2D CFD simulations were completed to analyse several competing VAWT farm configurations, alongside two hybrid configurations, both to find the highest performing design and also to further investigate the causes of this increase in performance. Further analyses were then run in order to investigate the local flow mechanisms that were producing these performance improvements and to consider how turbine solidity would affect the performance of the original optimised array.

While all of the proposed performance enhancing farm designs resulted in greater power output, the Staggered configuration showed a clear advantage which grew larger once the optimisation process was completed. The data gathered allowed for confirmation of the two flow mechanisms for VAWT performance enhancement which were found by Zanforlin [3] and the biomimetic shed vortex derived mechanism used by Whittlesey [7], alongside producing evidence for an additional mechanism, the Venturi effect. This enabled for a new design to be proposed which could offer an increase in array efficiency of 80% or greater compared to isolated turbines, where previously only 40% was considered to be possible. The 2-layer Staggered design showed the potential to have comparable performance with Mosetti's GA optimised HAWT farm, while having as little as one sixth of the footprint [10].

It is also shown that the solidity of the VAWT can have a significant impact on the flow mechanism which enables these performance enhancing farm designs to work, with higher solidity turbines allowing for the exploitation of the Venturi effect which results in much greater performance increases than the previously identified mechanisms. While the much larger blades will considerably increase the cost of a turbine, it is plausible that these efficiency enhancements would offset this in the long term by enabling greater lifetime power production.

5. References

[1] I. D. Brownstein, M. Kinzel, and J. O. Dabiri, "Performance enhancement of downstream vertical-axis wind turbines," J. Renew. Sustain. Energy, vol. 8, no. 5, p. 053306, Sep. 2016.

[2] S. H. Hezaveh, E. Bou-Zeid, J. Dabiri, M. Kinzel, G. Cortina, and L. Martinelli, "Increasing the Power Production of Vertical-Axis Wind-Turbine Farms Using Synergistic Clustering," Boundary-Layer Meteorol., vol. 169, no. 2, pp. 275–296, Nov. 2018.

[3] S. Zanforlin and T. Nishino, "Fluid dynamic mechanisms of enhanced power generation by closely spaced vertical axis wind turbines," Renew. Energy, vol. 99, pp. 1213–1226, Dec. 2016.

[4] J. Meyers and C. Meneveau, "Optimal turbine spacing in fully developed wind farm boundary layers," Wind Energy, vol. 15, no. 2, pp. 305–317, Mar. 2012.

[5] K. Beland, J. Bibeau, C. Gagnon, and J. Landry, "Offshore Wind Turbine Array."

[6] J. O. Dabiri, "Potential order-of-magnitude enhancement of wind farm power density via counter-rotating vertical-axis wind turbine arrays," J. Renew. Sustain. Energy, vol. 3, no. 4, p. 043104, Jul. 2011.

[7] R. W. Whittlesey, S. Liska, and J. O. Dabiri, "Fish schooling as a basis for vertical axis wind turbine farm design," Bioinspir. Biomim., vol. 5, no. 3, p. 035005, Sep. 2010.

[8] 4C Offshore, "Global Offshore Wind Speeds Rankings", 2019, Available: https://www.4coffshore.com/windfarms/windspeeds.aspx, [Accessed: 03- Apr- 2019].

[9] R. Lanzafame, S. Mauro, and M. Messina, "2D CFD Modeling of H-Darrieus Wind Turbines Using a Transition Turbulence Model," Energy Procedia, vol. 45, pp. 131–140, 2014.

[10] G. Mosetti, C. Poloni, and B. Diviacco, "Optimization of wind turbine positioning in large windfarms by means of a genetic algorithm," 1994.

[11] N. Bons, "Optimization of Vertical Axis Wind Turbine Farm Layout," Am. Inst. Aeronaut. Astronaut., pp. 1–8.

[12] T. J. Carrigan, B. H. Dennis, Z. X. Han, and B. P. Wang, "Aerodynamic Shape Optimization of a Vertical-Axis Wind Turbine Using Differential Evolution," ISRN Renew. Energy, vol. 2012, pp. 1–16, 2012.

[13] M. C. Claessens, "The Design and Testing of Airfoils for Application in Small Vertical Axis Wind Turbines," 2006.

[14] P. Delafin, T. Nishino, L. Wang, and A. Kolios, "Effect of the number of blades and solidity on the performance of a vertical axis wind turbine" Journal of Physics: Conference Series, Volume 753, 2016.

[15] M. A. Miller, S. Duvvuri, I. Brownstein, M. Lee, J. O. Dabiri, and M. Hultmark, "Vertical-axis wind turbine experiments at full dynamic similarity," J. Fluid Mech, vol. 844, pp. 707–720, 2018.

[16] L.A. Danao, J. Edwards, O. Eboibi, R. Howell, "A numerical investigation into the influence of unsteady wind on the performance and aerodynamics of a vertical axis wind turbine", Applied Energy, vol. 116, pp. 111-124, 1 March 2014.

[17] A-J Buchner, M.W. Lohry, L. Martinelli, J. Soria, A.J. Smits, "Dynamic stall in vertical axis wind turbines: Comparing experiments and computations", Journal of Wind Engineering and Industrial Aerodynamics, vol. 146, pp. 163-171, November 2015.

[18] F. Arpino, G. Cortellessa, M DellIsola, M. Scungio, V. Focanti, M. Profili, and M. Rotondi , "CFD simulations of power coefficients for an innovative Darrieus style vertical axis wind turbine with auxiliary straight blades", Journal of Physics Conference Series, Volume 923, Conference 1, 2017.

[19] A. Rezaeiha, I. Kalkman, and B. Blocken, "CFD simulation of a vertical axis wind turbine operating at a moderate tip speed ratio: Guidelines for minimum domain size and azimuthal increment," Renew. Energy, vol. 107, pp. 373–385, Jul. 2017.

[20] M. Ragheb and A. M., "Wind Turbines Theory - The Betz Equation and Optimal Rotor Tip Speed Ratio," in Fundamental and Advanced Topics in Wind Power, InTech, 2011.

[21] R. Howell, N. Qin, J. Edwards, N. Durrani, "Wind tunnel and numerical study of a small vertical axis wind turbine", Renewable Energy, Volume 35, Issue 2, pp. 412-422, February 2010.

[22] M. Raciti Castelli, A. Englaro, E. Benini, "The Darrieus wind turbine: proposal for a new performance prediction model based on CFD", Energy, Volume 36, Issue 8, pp. 4919-4934, August 2011.

[23] A. M. Chowdhury, H. Akimoto, and Y. Hara, "Comparative CFD analysis of Vertical Axis Wind Turbine in upright and tilted configuration,"

Renew. Energy, vol. 85, pp. 327–337, Jan. 2016.

[24] J. Bartl and L. Saetran, "Blind test comparison of the performance and wake flow between two in-line wind turbines exposed to different turbulent inflow conditions," Wind Energ. Sci, vol. 2, pp. 55–76, 2017.

[25] C. Desmond, J. Murphy, L. Blonk, and W. Haans, "Description of an 8 MW reference wind turbine," in Journal of Physics: Conference Series, 2016, vol. 753, no. 9.

[26] A. Inoue, R. Takahashi, T. Murata, J. Tamura, M. Kimura, M.-O. Futami, and K. Ide, "A calculation method of the total efficiency of wind generators," Electr. Eng. Japan, vol. 157, no. 3, pp. 52–62, Nov. 2006.

[27] N. Qin, R. Howell, N. Durrani, K. Hamada, and T. Smith, "Unsteady Flow Simulation and Dynamic Stall Behaviour of Vertical Axis Wind Turbine Blades," Wind Eng., vol. 35, no. 4, pp. 511–527, Aug. 2011.